scientific reports

Check for updates

OPEN

G protein-coupled receptor 91 activations suppressed mineralization in *Porphyromonas gingivalis*–infected osteoblasts

Wenqi Su[1,3], Dandan Zhang[1,3], Yujia Wang[1,3], Lang Lei[2] & Houxuan Li[1]✉

Succinate receptor GPR91 is one of the G protein-coupled receptors (GPCRs) that interacts with various proteins to regulate diverse cellular functions such as cell morphology, apoptosis, and differentiation. In this study, we investigated whether the GPR91-mediated signaling pathway regulates mineralization in *Porphyromonas gingivalis* (*P. gingivalis*)-treated osteoblasts and to determine its potential role in osteoclast differentiation. Primary mouse osteoblasts from wild-type (WT) and GPR91 knockout (GPR91$^{-/-}$) mice infected with *P. gingivalis* were used for in vitro experiments. The results showed that inhibition by 4C, a specific inhibitor, and GPR91 knockout promoted mineralization in *P. gingivalis*-infected osteoblasts. Surprisingly, GPR91 knockdown decreased the migration ability of osteoblasts. Moreover, compared with *P. gingivalis*-infected WT osteoblasts, GPR91$^{-/-}$ osteoblasts exhibited decreased RANKL production, and conditioned media (CM) from bacteria-infected GPR91$^{-/-}$ osteoblasts suppressed the formation of osteoclast precursors. Moreover, *P. gingivalis* mediated the role of GPR91 in osteoblast mineralization by activating the NF-κB pathway. These findings suggest that GPR91 activation reduces mineralization of *P. gingivalis*-infected osteoblasts and promotes osteoclastogenesis in macrophages. Therefore, targeting GPR91 may mitigate the loss of alveolar bone during bacterial infection.

Keywords GPR91, *P. gingivalis*, Osteoblasts, NF-κB, Mineralization

Chronic periodontal disease is an inflammatory disease which is characterized by damage to the tooth-supporting tissue. The disease is mainly caused by the imbalance between the parasitic flora and the host's defense system[1]. Anaerobic bacteria can damage tissues by increasing the production of inflammatory cells, damaging collagen fibers and the alveolar bone[2]. The alveolar bone exists in a dynamic state, influenced by the balance between wound healing and bone loss[3]. The immune system in the affected sites tdisrupts the ratio between bone formation and resorption, ultimately causing bone loss[4].

Osteoblasts are mostly specialized bone-forming cells known to regulate the metabolism of alveolar bone. The degradation of alveolar bone, a hallmark of periodontitis, is mainly driven by the excessive activation of osteoclast precursors and production of mature osteoclasts[5]. Alveolar bone destruction due to bone resorption may lead to developmental abnormalities of the bones[6]. The differentiation of osteoblast lineages is inhibited in an inflammatory environment.

Porphyromonas gingivalis (*P. gingivalis*) is a Gram-negative anaerobic pigmented coccobacillus which grows well in an anaerobe state, establishing colonies in the periodontal pockets. It also penetrates deeply into tissues and bone tissue[7]. *P. gingivalis* can generate many virulent factors, such as lipopolysaccharide (LPS), hemagglutinin, and gingipain[8]. Bacterial cells, fimbriae and LPS are recognized by pattern recognition receptors, notably Toll-like receptor 2 and 4, while metabolites produced by *P. gingivalis* and host cells are recognized by various G-protein-coupled receptors (GPRs) on the cell membrane[9]. It has been shown that butyric acid regulates the GPR41 signaling pathways[10], *P. gingivalis* protease activates the protease-activated receptor (PAR), a G protein-coupled receptor, belonging to a unique class of GPRs[11]. The ligand binding activates several signaling

[1]Department of Periodontics, Nanjing Stomatological Hospital, Affiliated Hosptital of Medical School, Institute of Stomatology, Nanjing University, 30 Zhongyang Road, Nanjing, Jiangsu 210008, People's Republic of China. [2]Department of Orthodontics, Nanjing Stomatological Hospital, Affiliated Hosptital of Medical School, Institute of Stomatology, Nanjing University, Nanjing, People's Republic of China. [3]Central Laboratory of Stomatology, Nanjing Stomatological Hospital, Affiliated Hosptital of Medical School, Institute of Stomatology, Nanjing University, Nanjing, People's Republic of China. ✉email: lihouxuan3435_0@163.com

molecules and causes conformational changes in the receptor, triggering biological responses such as migration, proliferation, and cell division[12].

Succinate receptor 1 (SUCNR1) is a G protein-coupled receptor also known as GPR91. Studies have shown that it is deregulated in various inflammatory diseases. Several ligands that activate GPR91 through a coordination compound signal transduction cascade have been reported, and this activation causes the release of inflammatory markers. In mice with arthritis, GPR91 knockout alleviated the symptoms of rheumatoid arthritis in bone[13]. Guo et al. found that under high glucose conditions and succinate concentration, the expression of the SUCNR1 was increased, promoting osteoclast formation and enhancing osteoclastogenesis[14]. Previous studies demonstrated that application of SUCNR1 antagonists directly to the affected area or SUCNR1 knockdown stimulated inflammatory signaling and decreased osteoclast formation in vivo in a mouse model of *Fusobacterium nucleatum* (*F. nucleatum*)-induced periodontitis[15]. However, the impact of GPR91 on the mineralization of osteoblasts in an inflammatory environment is poorly understood. Therefore, we aimed to investigate the role of GPR91 in osteoblast calcification following *P. gingivalis* infection.

Result

P. gingivalis infection promoted GPR91 expression and inhibited mineralization in osteoblasts

To investigate the impact of *P. gingivalis* on osteoblasts, cells were incubated with different concentrations of *P. gingivalis* at the multiplicity of infection (MOI) of 10, 50, and 250 for 24 h. The results showed that the expression level of pro-inflammatory cytokine IL-6 levels was progressively increased with the incremental increase in MOI. In contrast, the expression of osteogenic-related genes Osterix (OSX), runt-associated transcription factor (RUNX) 2, and osteopontin (OPN) was decreased (Fig. 1A). Western blot analysis at the two-day time point revealed that the expression of osteogenesis-related proteins was significantly reduced (Fig. 1B and Supplemental Information S1).

Based on the above results, *P. gingivalis* treatment at an MOI of 50 was selected for further tests. Subsequently, results of the alkaline phosphatase (ALP) staining conducted at seven days (Fig. 1C) and the alizarin red S (ARS) staining performed at 14 days (Fig. 1D) revealed that mineralization capacity of osteoblasts was decreased following *P. gingivalis* treatment. The link between minerality-related markers and GPR91 exhibited an inverse relationship. Consequently, cells were cultured in the mineralization induction medium for different times in the absence of *P. gingivalis*. Interestingly, a positive correlation was observed between the duration of induction and upregulation for OSX, RUNX2, and OPN (Fig. 1E&F and Supplemental Information S1). However, the expression of GPR91 was downregulated (Fig. 1E).

Blocking GPR91 alleviated the inhibitory effect of *P. gingivalis* on mineralization of osteoblasts

To clarify the function of GPR91 in osteoblast mineralization, in vitro experiments were conducted using 4C, a selective inhibitor of GPR91, in conjunction with osteoblasts extracted from GPR91$^{-/-}$ mice. The cells were subjected to different pre-treatments of various dosages of 4C in a controlled laboratory setting, and the cellular activity was determined using the Cell Counting Kit 8 (CCK8) following administration of 4C to minimize any interference caused by the chemical medication. The optimal concentration of 5 μM was selected depending on the drug's effect on cell activity and inhibitory effects on GPR91 (Fig. 2A). Before *P. gingivalis* stimulation, osteoblasts extracted from WT mice were incubated with 4C for 2 h. This caused a significant increase in the expression of OSX, RUNX2, and OPN after 24 h of bacterial stimulation, whereas IL-6 expression was decreased (Fig. 2B). Moreover, the protein expression of osteogenic genes was determined 2 days after treatment with Western blotting. Under inflammatory conditions, the mineralization ability of osteoblasts was significantly boosted due to the inhibition of GPR91 (Fig. 2C and Supplemental Information S1). Similar results were observed in the ALP staining performed seven days later (Fig. 2D) and ARS staining conducted at 14 days (Fig. 2E).

To further verify the inhibitory effect of the GPR91 activity, qPCR and western blot analyses were performed to quantify the expression of mineralization-related markers and IL-6 in osteoblasts incubated with *P. gingivalis*. These assays were conducted on WT mice and animals lacking the GPR91 gene (Fig. 3A&B and Supplemental Information S1). Osteoblasts derived from GPR91$^{-/-}$ mice exhibited enhanced mineralization capacity and lower levels of inflammation. Similar observations were made in the ALP staining assay after seven days (Fig. 3C) and ARS staining assay after 14 days (Fig. 3D).

GPR91 promotes osteoclast differentiation under inflammatory conditions

To investigate whether GPR91 regulates osteogenic mineralization and osteoclast formation, cells extracted from the WT and GPR91$^{-/-}$ mice were incubated with *P. gingivalis*, and the CM were collected from these osteoblasts to treat osteoclast precursors. After 24 h of culture, the RANKL expression in the *P. gingivalis*-treated GPR91$^{-/-}$ osteoblasts was decreased (Fig. 4A&B and Supplemental Information S1). Moreover, the mRNA level of osteoclast marker genes (such as tartrate-resistant proton donor phosphatase (*TRAP*), *Nfatc1, CTSK, c-Fos,* and *Car2*) was markedly reduced following incubation with *P. gingivalis*-treated GPR91$^{-/-}$ mice osteoblastic CM (Fig. 4C). Furthermore, the CM obtained from *P. gingivalis*-treated GPR91$^{-/-}$osteoblasts formed the smallest number of osteoclasts compared with those induced by CM from *P. gingivalis* (Fig. 4D). The expression of the TRAP protein was increased in osteoclast precursors in the CM collected from infected GPR91$^{-/-}$ osteoblasts as shown in Fig. 4E and Supplemental Information S1.

GPR91 partially enhances osteoblast migration

Osteoblast surface receptors facilitate cell attachment and polarization, triggering osteoblast migration[16]. G protein-mediated signaling regulates the transmission of information across membranes. It promotes the

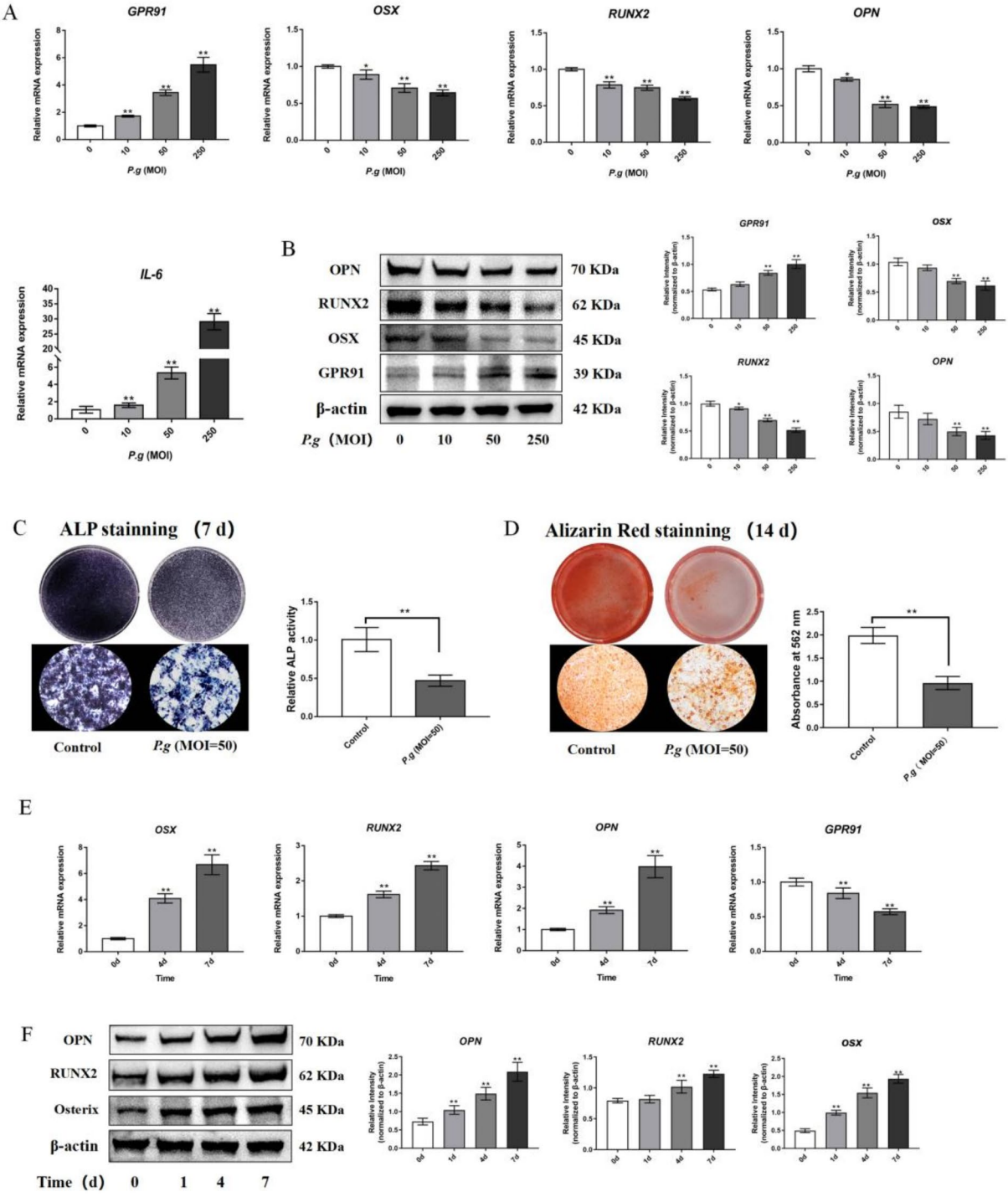

Fig. 1. *P. gingivalis* infection promoted GPR91 expression with inhibited mineralization in osteoblasts. Osteoblasts were cultured with different multiplicity of infections (MOIs) of *P. gingivalis*, and the expressions of OSX, RUNX2, OPN and IL-6 were detected by real-time PCR for 24 h (**A**) and western blotting after 48 h stimulation (**B**). ALP staining (**C**) was performed at 7 days, and ARS (**D**) was performed at 14 days after being stimulated with *P. gingivalis* at a MOI of 50. Expressions of mineralization-related markers and GPR91 in osteoblasts cementogenic-differentiated at 0, 4, and 7 days were examined by qPCR (**E**) and western blotting (**F**). In all cases, bars in graphs represent mean ± SEM. β-actin was adopted as an internal reference. *, $p < 0.05$; **, $p < 0.01$ compared with the Control.

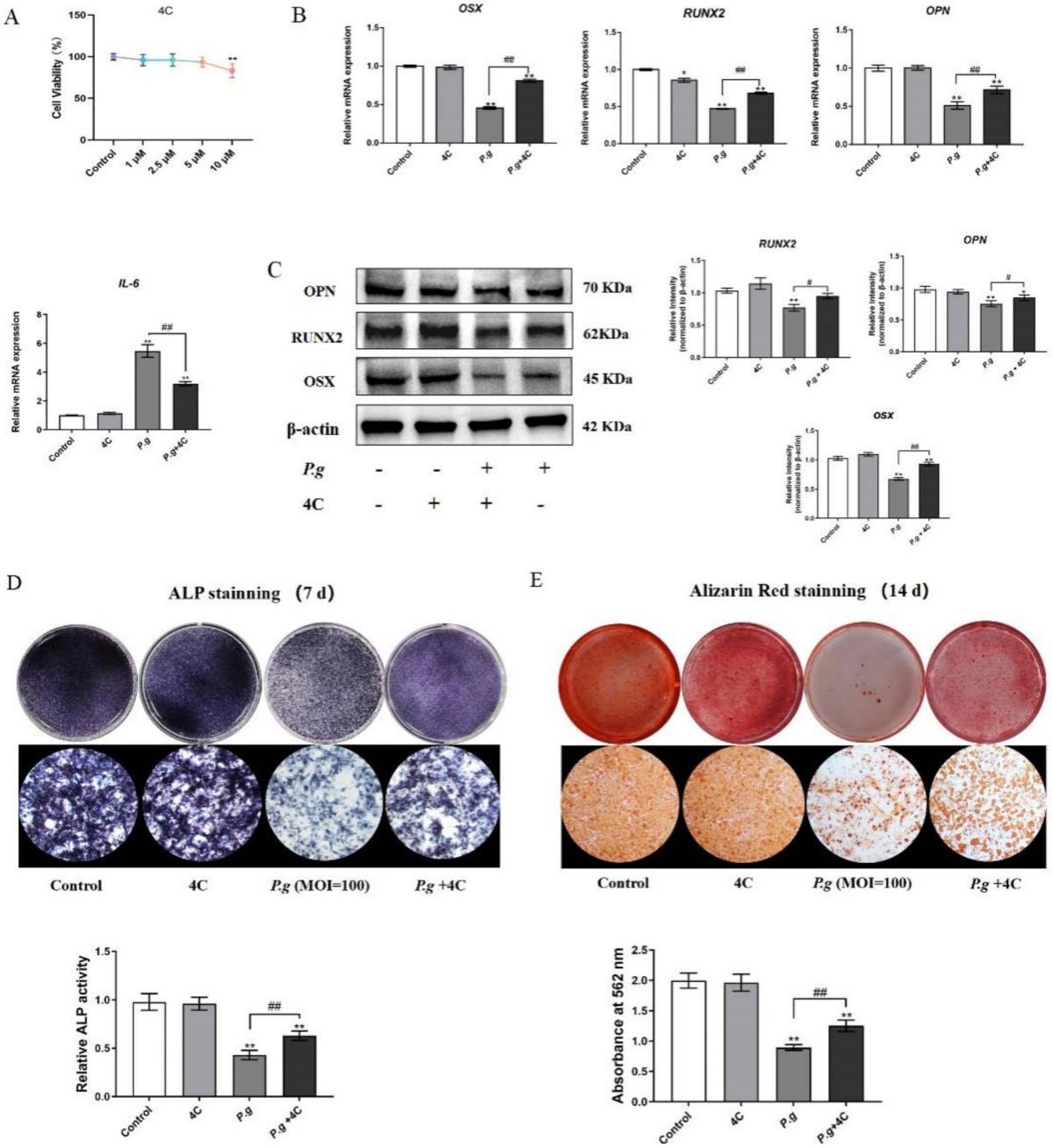

Fig. 2. Blocking GPR91 mitigated the bone mineralization inhibited by *P.gingivalis*. CCK8 examined the activity of osteoblasts treated with 4C at different concentrations (**A**). Osteoblasts were pretreated with 4C (5 μM) for 2 h and then treated with *P. gingivalis* at a MOI of 50. Gene transcript levels of OSX, RUNX2, OPN and IL-6 were analyzed by real-time PCR at 24 h (**B**) and protein levels were detected by western blotting after 48 h stimulation (**C**). ALP staining and ALP activity assay at 7 days (**D**) and ARS at 14 days (**E**) of osteoblasts treated with *P. gingivalis* at a MOI of 50. In all cases, bars in graphs represent mean ± SEM. β-actin was adopted as an internal reference. *, $p < 0.05$; **, $p < 0.01$ compared with the Control; #, $p < 0.05$; ##, $p < 0.01$ compared with the *P. gingivalis*-treated group.

recognition of external signals and their coupling with internal cellular information[17]. The WT and GPR91$^{-/-}$ osteoblasts were exposed to *P. gingivalis* for 24 h and then incubated in 6-well plates. Some were placed in a 24-well transwell culture chamber in the upper compartment. There were noticeable differences in the healed/damaged area ratio between osteoblasts from GPR91$^{-/-}$ mice and osteoblasts from WT mice, but the ratio was lower in the former (Fig. 5A). Results of the transwell experiments demonstrated that osteoblasts derived from WT mice exhibited increased migration after 24 h (Fig. 5B). Further analysis revealed a significant downregulation in

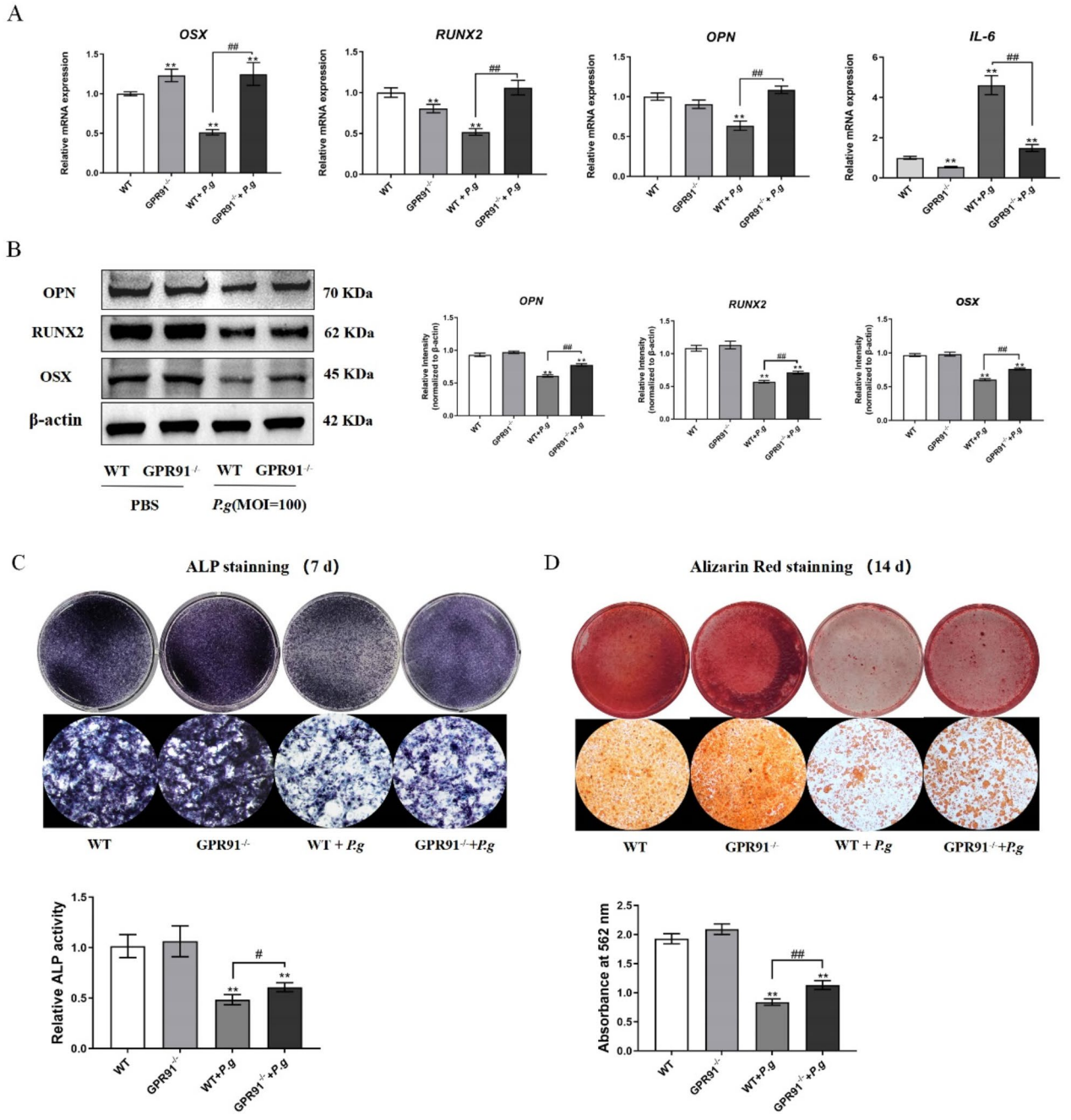

Fig. 3. GPR91 knockdown mitigated the bone mineralization inhibited by *P.gingivalis*. Osteoblasts from WT and GPR91$^{-/-}$ mice were stimulated with *P. gingivalis* (MOI = 50). Gene transcript levels of OSX, RUNX2, OPN and IL-6 were analyzed by real-time PCR for 24 h (**A**), and protein levels were detected by western blotting after 48 h stimulation (**B**). ALP staining and ALP activity assay at 7 days (**C**) and ARS at 14 days (**D**) of osteoblasts treated with *P. gingivalis* at a MOI of 50. In all cases, bars in graphs represent mean ± SEM. β-actin was adopted as an internal reference. *, $p < 0.05$; **, $p < 0.01$ compared with the WT group; #, $p < 0.05$; ##, $p < 0.01$ compared with the WT + *P. g*-treated group. The WT group served as the Control group.

matrix metalloproteinases (MMP)2, MMP9, and chemokine ligand (CCL)2 transcription levels in osteoblasts from GPR91$^{-/-}$ mice compared with those from WT mice (Fig. 5C). This finding was corroborated by western blotting analysis of the protein expression (Fig. 5D and Supplemental Information S1). Altogether, these results indicated that GPR91 played a significant role in cell migration.

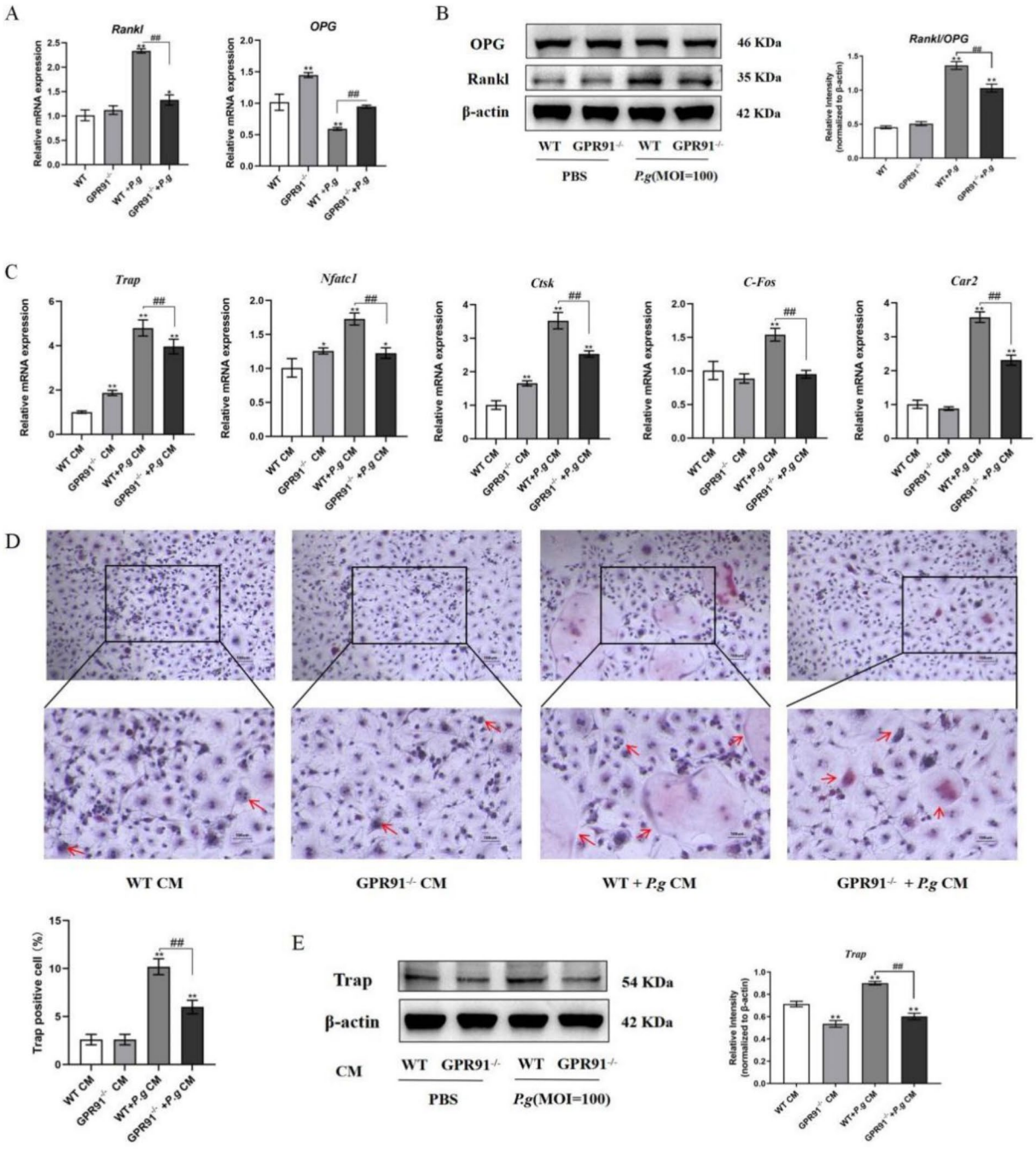

Fig. 4. Conditioned medium from GPR91-knockdown osteoblasts inhibited Osteoclastogenesis. Osteoblasts from WT and GPR91$^{-/-}$ mice were stimulated with *P. gingivalis* (MOI = 50) for 24 h or 48 h. Gene transcript levels of RANKL and OPG were analyzed by real-time PCR (**A**), and protein levels were detected using western blotting (**B**). The mice BMMs were treated with the CM of osteoblasts from WT and GPR91$^{-/-}$ mice stimulated by *P. gingivalis* (MOI = 50) for 24 h. (**C**) After 3 days of culture, the relative mRNA expression of osteoclast markers in osteoclasts was detected by real-time PCR. (**D**) After 5 days of culture, the formation of osteoclasts was analyzed by Trap staining, and the number of osteoclasts was counted as Trap positive multinucleated cells. (**E**) Trap protein levels in differentiated BMMs were detected after culture for 3 days. In all cases, bars in graphs represent mean ± SEM. β-actin was adopted as an internal reference. *, $p < 0.05$; **, $p < 0.01$ compared with the WT CM group; #, $p < 0.05$; ##, $p < 0.01$ compared with the WT + *P. g* CM group. The WT CM group served as the Control group.

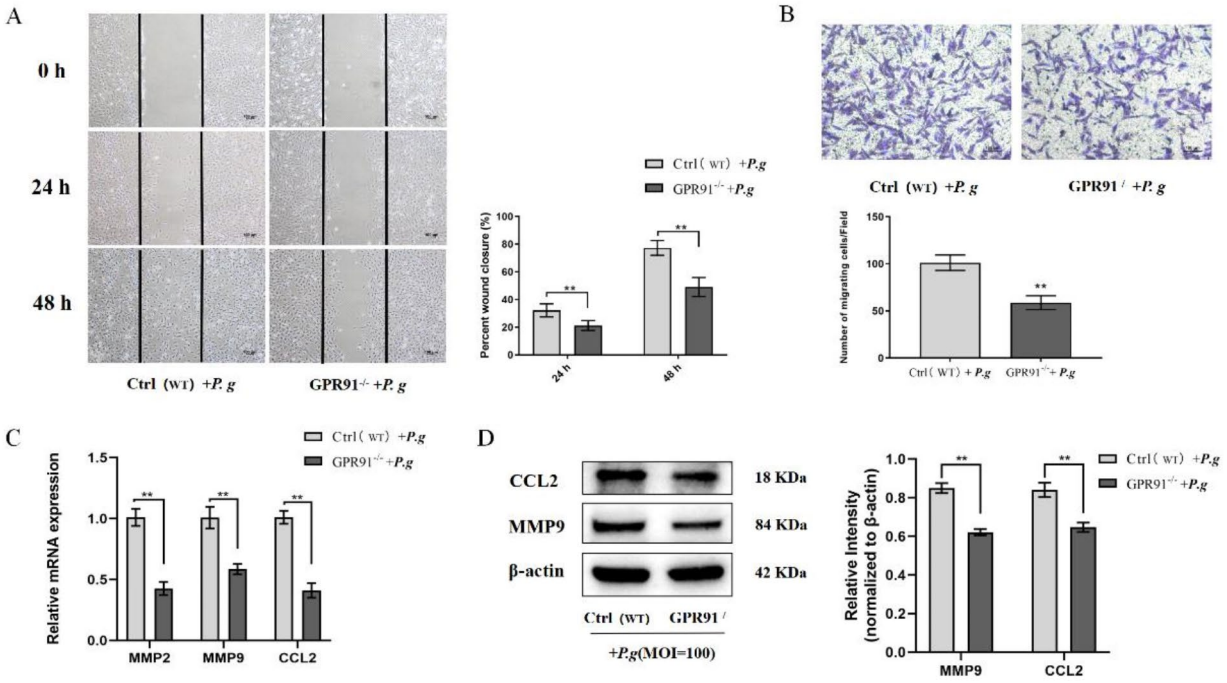

Fig. 5. Involvements of GPR91 in *P. gingivalis*-induced osteoblasts migration. Osteoblasts from WT and GPR91$^{-/-}$ mice were stimulated with *P. gingivalis* (MOI = 50) for 24 h and inoculated in 6-well culture plates and the upper compartment of a 24-well trans-well culture chamber. (**A**) Wound healing migration test. The wound surface was recorded with a microscope immediately after scratching (0 h) and migrated for 24 and 48 h. (**B**) Transwell migration test. After 24 h, the cell migration was observed with a microscope. Scale = 100 μm. Osteoblasts from WT and GPR91$^{-/-}$ mice were stimulated with *P. gingivalis* (MOI = 50) for 4 h or 24 h. Gene transcript levels of MMP2, MMP9 and CCL2 were analyzed by real-time PCR (**C**) and protein levels were detected by western blotting (**D**). In all cases, bars in graphs represent mean ± SEM.*, $p < 0.05$; **, $p < 0.01$ compared with the Ctrl (WT) + *P.g*-treated group.

P. gingivalis mediates GPR91 involvement in osteoblast mineralization through activation of NF-κB pathway

To elucidate the potential mechanism mediating the GPR91-facilitated osteoblast mineralization, we explored various signaling pathways. Western blotting indicated that p-ERK1/2/total-ERK1/2 and p-P65/total-P65 were upregulated following treatment with *P. gingivalis*. However, the expression of p-P38/total-P38 and p-JNK/ total-JNK was not significantly affected (Fig. 6A and Supplemental Information S1).

The osteoblasts were pretreated with specific inhibitors of the ERK1/2 pathway, SCH772984, and P65 pathway inhibitor, SC75741. Notably, inhibition of the ERK pathway increased the expression of OPN. However, it did not reverse the expression levels of OSX and RUNX2, and did not downregulate GPR91 expression (Fig. 6B and Supplemental Information S1). Besides, inhibition of the P65 pathway not only prevented GPR91 overexpression but also enhanced the mineralization process following *P. gingivalis*. This enhancement was evidenced by increased OSX, RUNX2, and OPN expression (Fig. 6C and Supplemental Information S1). GPR91 regulates the mineralization of osteoblasts via the P65 signaling pathway.

Discussion

Accumulation of bacteria such as *P. gingivalis*, *Tannobacteria forsythiae*, and *Treponemas* around the teeth causes degeneration of the alveolar bone[18]. *P. gingivalis* is the main bacterium contributing to the development periodontal diseases. Evidence from previous studies shows that many *P. gingivalis* strains inhibit osteoblasts, which delays alveolar bone growth. Studies have shown that LPS, lipids, metabolites, and ultrasound extracts from *P. gingivalis* can decrease the osteoblast differentiation and osteogenesis[19–22]. Therefore, an animal model of periodontitis induced by inoculation with live *P. gingivalis* was established and found to be similar to the human patient model[23]. In a mouse model of periodontitis, *P. gingivalis* could enter the infected cells (gingival epithelial cells, fibroblasts, osteoblasts, osteoblasts) at the infected site[24]. This resulted in the destruction of osteoblasts and osteoclasts, inhibiting the osteoblast pool and causing bone loss. Taken together, analysis of the total bacteria revealed its functional advantages and simulate pathological processes in vivo. In this study, researchers used *P. gingivalis* was directly applied to osteoblasts rather than using its components (such as LPS).

Sex hormones exert pleiotropic effects on several tissues and organs, which promotes bone formation, homeostasis, and immunological function[25]. In this study, osteoblasts were extracted from a 3-day newborn

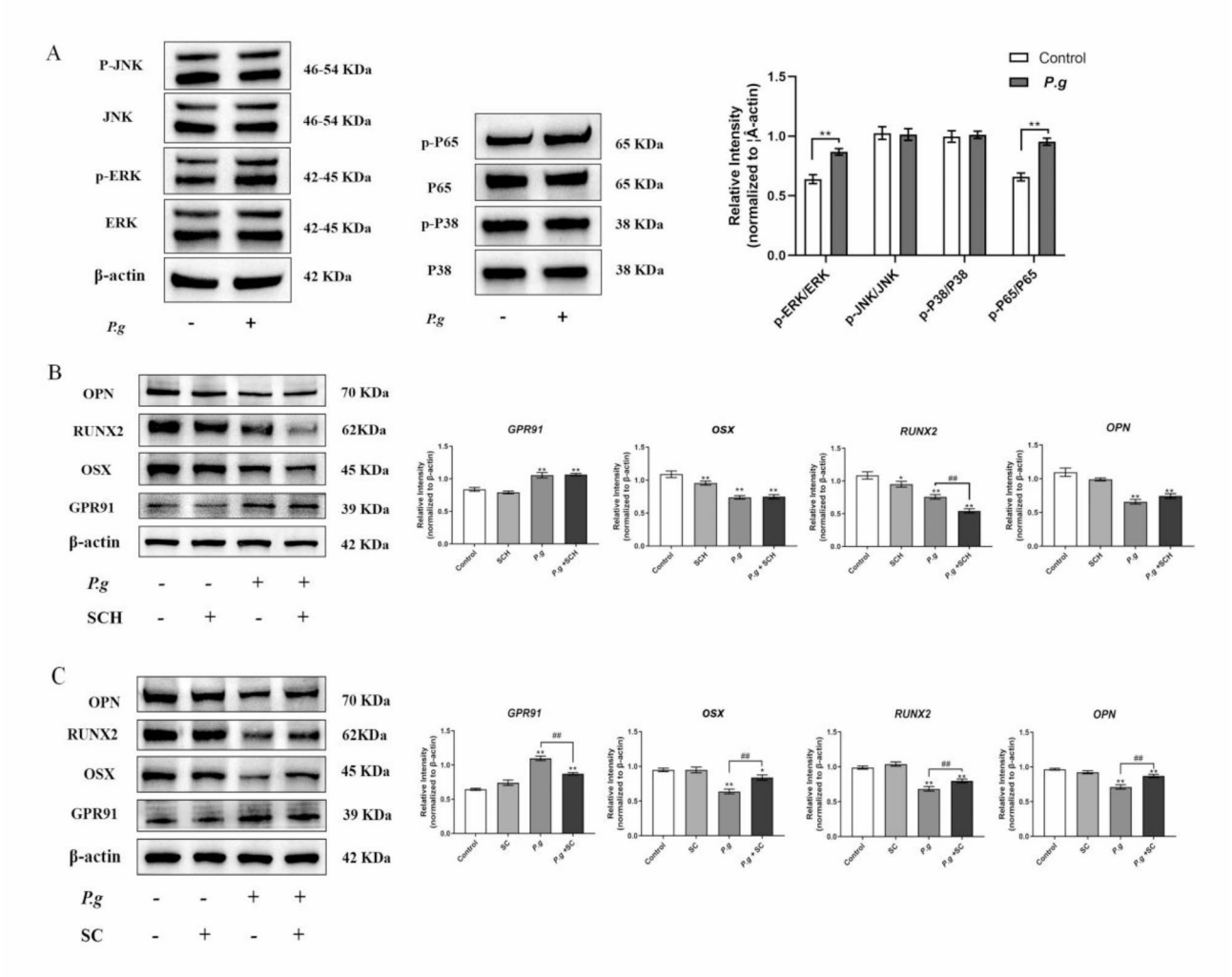

Fig. 6. GPR91-NFκB signalling pathway was involved in the mineralization of osteoblasts under inflammation. (**A**) Osteoblasts from WT mice were treated with *P. gingivalis* (MOI = 50) for 1 h and harvested for western blotting to reveal the phosphorylation of NF-κB and MAPK pathways. Osteoblasts were pretreated with SCH772984 (ERK inhibitor, 500 nM) and SC75741 (P65 inhibitor, 5 μM) and then treated with *P. gingivalis* (MOI = 50) for 48 h. Protein levels of OSX, RUNX2, OPN and GPR91 were detected by western blotting (**B**&**C**). In all cases, bars in graphs represent mean ± SEM. *, $p < 0.05$; **, $p < 0.01$ compared with the Control group; #, $p < 0.05$; ##, $p < 0.01$ compared with the *P. g*-treated group.

male mice, and therefore, the effects of sex hormones might be minimal. Given that large epidemiological studies have demonstrated that periodontal disease risk and progression/severity are higher in men than in women, even after controlling for all major covariates[26], studies using male and female animals are advocated to determine whether sex differences exist in the effect of succinate-GPR91 axis.

The precise function of GPR91 in regulating periodontitis following succinate pre-treatment remains unknown, although studies have demonstrated its ability to stimulate osteoclast production[14,27]. In this study, we investigated the regulatory effects of GPR91 on mineralization of osteoblasts treated with *P. gingivalis*. IL-6, a cytokine with many effects, is widely recognized for its effects in the production of osteoclasts and inhibition of ALP and collagenase production in osteoblasts[28]. Therefore, we measured IL-6 expression to confirm the establishment of an inflammatory environment in vitro, which exhibited a positive correlation with the concentration of *P. gingivalis* stimulation (Fig. 1).

Several protein–protein interactions contribute to the activation of several signaling molecules, forming a complex signaling network that regulates the crucial process of osteoblast development, which is essential for bone production. RUNX2 is expressed in preosteoclasts, immature osteoblasts, and has been reported to modulate osteoblast phenotypes and bone formation[29]. RUNX2 alters the differentiation of several genes related to bone matrix proteins, including OPN and osteocalcin[30]. OPN is an extracellular matrix glycoprotein that influences bone remodeling and is expressed preferentially in the intermediate phase of bone formation[31]. OSX is a zinc-finger-containing transcription factor and an essential player in osteoblastogenesis, acting downstream target of RUNX2[32]. The present results showed that with the progressive worsening of the inflammation induced

by *P. gingivalis*, the expression of GPR91 was increased accompanied by a gradual decrease in the expression of OSX, RUNX2, and OPN (Fig. 1).

Consequently, we analyzed the effects of GPR91-mediated signaling on osteoblast mineralization in an inflammatory environment by measuring the expression of OSX, RUNX2, and OPN using GPR91$^{-/-}$ osteoblasts treated with *P. gingivalis*. Notably, GPR91 knockdown restored the mineralization of osteoblasts exposed to *P. gingivalis*, as shown in Figs. 2 and 3. Inflammation in this study was detected at the cellular level in vitro, and subsequent experiments were performed using the 4C inhibitor and gene knockout mice.

Chronic periodontitis occurs due to the continuous breakdown and formation of alveolar bone, which is influenced by the ratio of RANKL to OPG. A high RANKL/OPG ratio causes active breakdown of alveolar bone[33]. Studies have demonstrated that live *P. gingivalis* contribute to the production of RANKL by osteoblasts[34]. RANKL is a cytokine that promotes the formation of osteoclasts, reducing bone tissue[35]. Osteoblasts regulate the production of osteoclasts in normal bone tissue by producing two opposing factors, RANKL and OPG. The equilibrium between RANKL and OPG is crucial for the maintenance of the bone density in the alveolar bone. In this study, we found that GPR91 knockout alleviated the increase in RANKL expression in osteoblasts following exposure to *P. gingivalis* (Fig. 4A&B).

In addition, the culture medium of infected osteoblasts and GPR91 knockout cells was used to treat osteoclast precursor cells. The results indicated that the culture medium decreased the formation of osteoclasts from their precursors compared to the culture medium from wild-type osteoblasts infected with bacteria (Fig. 4D&E). Succinate treatment increased the number of osteoclasts in bone marrow cell cultures and stimulated the expression of marker genes for osteoclast differentiation and maturation[36]. Treatment with the SUCNR1-specific antagonist 4C triggered osteoclast formation, while the succinate-induced osteoclast formation was abolished in osteoclasts derived from SUCNR1 knockout mice[14]. Altogether, these results demonstrated that GPR91 participated in osteoblast secretion under inflammatory conditions and promoted osteoclast differentiation.

The processes of bone formation and regeneration are highly dependent on the migration and adhesion characteristics of osteoblasts[37]. In our previous study, we found that GPR91 augmented the migratory capacity of periodontal ligament fibroblasts under low oxygen conditions[38]. Analysis of GPR91-deficient mice models revealed a significant suppression of dendritic cell secretion and migration[27]. MMP promoted the migration of various cells in processes, such as wound healing and bone remodeling[39]. Inhibition of the MMP13 activity was found to increase cell mineralization while decreasing cell migration[40]. MMP9 and MPP2 are well-established proteins involved in the regulation of cell migration, which, when decreased, results in suppressed cell migration[41].

CCL2 is a known chemoattractant that modulates the migration, proliferation, and cancer cell invasion. It has also been implicated the osteoclastogenesis process. Silencing CCL2 enhanced bone mineral density[41]. Interestingly, we found that although GPR91 knockout could partially restore the mineralization ability of osteoblasts which was inhibited by *P. gingivalis*, it suppressed the migration ability of osteoblasts and the expression of MMP2, MMP9, and CCL2 (Fig. 5). A study by Ko SH et al. showed that succinate activated Gαq, Gαi and Gα12, and Gαq and Gα12 in human marrow mesenchymal stem cells (hMSC), thereby stimulating their migration[42]. In this study, we hypothesized that *P. gingivalis*-stimulated osteoblasts exhibited intracellular succinate accumulation accompanied with increased Gαq and Gα12 activity to promote osteoblast migration.

Available evidence indicates that NFκB and MAPK pathways influence the GPR9 signaling pathway[14,42,43]. NFκB pathway is a classic inflammatory pathway. Activation of the mitogen-activated (MAP) kinases pathway (comprising the crucial ERK1/2, JNK, and p38) was found to induce osteogenic differentiation[44–46]. The ERK pathway is a member of the MAPK signaling pathways. Studies have shown that important signaling molecules that control osteoblast activity work by activating the ERK pathway[47]. Studies have shown that ERK enhances cell proliferation, augments RUNX2 transcriptional activity, and facilitates osteogenic diversity[46]. Activation of JNK participates in the development of human periosteal osteoblasts in an in vitro system[44]. Upregulation of SUCNR1 expression can activate MAP kinases, specifically ERK 1/2, in several cellular models, such as HEK293 cells and immature dendritic cell models under in vitro conditions[48].

Following stimulation *P. gingivalis*, we performed a more in-depth analysis of the MAPK and P65 pathways. The results showed that the ERK and P65 pathways were activated in *P. gingivalis*-stimulated cells (Fig. 6A). In this study, we examined the functions of the ERK and P65 pathways using inhibitors that specifically target ERK and P65, respectively. Inhibition of the P65 pathway upregulated the mineralization capacity of osteoblasts in an inflammatory environment and, downregulated the expression of GPR91 (Fig. 6C). Succinate stimulates the SUCNR1 to increase P65 and P50 expression in osteoclast cells[14]. This triggers the release of RANKL and the formation of osteoclasts. We hypothesized that activation of the NF-κB pathway by *P. gingivalis* may alter GPR91 thereby influence osteoblast mineralization and osteoclast development.

Despite the important findings in this study, there are some limitations that should be acknowledged. Firstly, we did not investigate the overall GPR activation in this study, and only focused on the effect of GPR91 in osteoblasts mineralization. There are several questions regarding the functions of GPR91 that remain to be answered, such as whether succinate, an agonist of GPR91, has the same effect *as P. gingivalis*, and whether GPR91 participates in multiple bacterial infection, including *F. nucleatum* and *Prevotella intermedia*. Although we observed that GPR91 activation in *P. gingivalis*-stimulated osteoblasts may promote osteoclastogenesis, a mice periodontitis model may shed further light on the overall effects of GPR activation.

Conclusion

Activation of GPR91 decreased mineralization and increased macrophage osteoclastogenesis in *P. gingivalis*-infected osteoblasts. The results suggested that GPR91 played a central part in the modulation of osteoblast function, partly through the NF-κB signaling pathway. On the other hand, inhibition of osteoblast GPR91

decreased the inhibitory effect of *P. gingivalis* and presents a new approach for repairing and regenerating bone damage induced by *P. gingivalis*.

Materials and methods

Osteoblast isolation and culture

Osteoblasts were separated from neonatal male GPR91$^{-/-}$ and C57BL6/J WT mice (GemPharmatech Co. Ltd., Nanjing, China). The calvaria bones of neonatal mice were cut off and cultured by trypsin and collagenase digestion method as we described previously[49]. Cells obtained from digestion were cultured at 37℃ in 5% CO2 in α-MEM with 10% fetal bovine serum (FBS), 100 mg/ml streptomycin, and 100 U/ml penicillin. Observe and follow up after approximately 3–5 generations of culture once the cell density reaches 80%. Visible osteoblasts were observed one week after staining with the BCIP/NBT ALP color development kit (Beyotime, China). After 14 days of culture, calcium accumulation was assessed using alizarin red staining (Sigma-Aldrich, USA). To test whether osteoblasts could produce a mineralized matrix, cells were in a medium containing 10 mM β-glycerophosphate, 50 μM ascorbic acid, and 0.1 μM dexamethasone with α-MEM supplemented with 10% FBS. The osteogenic medium was changed daily.

Bacteria culture and drug treatment

P. gingivalis (ATCC33277) developed in a Brain Heart Infusion (BHI) medium, adding 0.1% yeast extract, 1 μg/ml vitamin K1, and hemin of 5 μg/ml. The visual density for the bacterial spread out was estimated with a spectrophotometer around 600 nm. An OD of 1 corresponds to a concentration of 10^9 *P. gingivalis*/ml.

Osteoblasts were infected with live *P. gingivalis* at the MOI of 10, 50, and 250. The concentration of the inhibitor was 5 μM. The inhibitor used is 4C, which is a selective inhibitor for GPR91. The ERK inhibitor SCH772984 and the P65 inhibitor SC75741 are introduced at 500 nM and 5 μM, respectively. Additionally, osteoblasts were pretreated with the drug for 2 h before stimulation by *P. gingivalis*.

Isolation of RNA and quantitative PCR

Osteoblasts to be lysed were treated with RNA extraction reagent ((Accurate Biology, China). A Nanodrop (Thermo Fisher Scientific, USA) calculated the total molarity of RNA. The PrimerScriptTM RT kit from Vazyme was used for reverse engineering. Real-time PCR of the reverse-engineered samples was done by employing SYBR Green Master MIX (Vazyme, China). The qPCR primers were then synthesized using PrimerBank's design code (https://pga.mgh.harvard.edu/primerbank/). The pattern of primers used is shown in Table 1. Relative quantification was achieved using the comparative $2^{-\triangle\triangle}$Ct method.

Alkaline phosphatase (ALP) activity and staining

The ALP staining procedure was done with a BCIP/NBT Staining Kit (Beyotime, China). The cells were stimulated to undergo osteogenic differentiation and treated with 4% paraformaldehyde for 30 min on the 7 days. Subsequently, they were placed in a BCIP/NBT staining solution for a suitable duration under dark conditions. The ALP activity testing was conducted using the ALP activity assay kit (Beyotime, China) following the methods provided by the producer.

Alizarin red S (ARS) staining

The cells were incubated within osteogenic medium for 14 days, then treated with 4 percentage paraformaldehydes for 30 min to fix them. Subsequently, the cells were stained with ARS for a further 30 min. The development of mineralized nodules by the osteoblasts was evaluated using ARS staining. The calculation of absorbance at

Genes	Sequence(5'-3')	Sequence(3'-5')
GPR91 (mouse)	CTTGTGAGAATTGGTTGGCAA	CATCTCCATAGGTCCCCTTATCA
OSX (mouse)	CTTCCCAATCCTATTTGCCGTTT	CGGCCAGGTTACTAACACCAATCT
RUNX2 (mouse)	CATTTGCACTGGGTCACACGTA	GAATCTGGCCATGTTTGTGCTC
OPN (mouse)	GATGATGATGACGATGGAGACC	CGACTGTAGGGACGATTGGAG
IL-6(mouse)	AGTTGCCTTCTTGGGACTGA	TCCACGATTTCCCAGAGAAC
RANKL (mouse)	AGCCGAGACTACGGCAAGTA	AAAGTACAGGAACAGAGCGATG
OPG(mouse)	ACCCAGAAACTGGTCATCAGC	CTGCAATACACACACTCATCACT
TRAP(mouse)	TGTGAGGGAGGAGGCGTCTGC	CGTTCCCAAGAAAGCTCTACC
NFATc1(mouse)	CCGTCACATTCTGGTCCATAC	CCAATGAACAGCTGTAGCGTG
Ctsk(mouse)	GTGTCCATCGATGCAAGCTTGGCA	GCTCTCTCCCCAGCTGTTTTTAAT
c-Fos(mouse)	CGGGTTTCAACGCCGACTA	TTGGCACTAGAGACGGACAGA
Car2(mouse)	TCCCACCACTGGGGATACAG	CTCTTGGACGCAGCTTTATCATA
MMP2 (mouse)	CGATGTCGCCCCTAAAACAG	GCATGGTCTCGATGGTGTTC
MMP9 (mouse)	GGAGACGCCACGCATTTCA	CTTACGGCCTGAGGGTCTTG
CCl2 (mouse)	AACTGCATCTGCCCTAAGGT	GGCATCACAGTCCGAGTCA
β-actin (mouse)	AGGTCGGTGTGAACGGATTTG	TGTAGACCATGTAGTTGAGGTCA

Table 1. The primer sequences used for real-time qPCR.

a wavelength around 405 nm was recorded, and the ARS standard curve was applied to determine the ARS amount.

Osteoclastogenesis by the conditioned medium from osteoblasts

Similarly, osteoblasts obtained from the tibia of GPR91$^{-/-}$ and WT mice were cultured for 24 h in the availability or negativity of *P. gingivalis*. Then, the medium of osteoblasts as a CM was collected to generate osteoclasts. Bone marrow cells from 6-week-old mice (GemPharmatech Co. Ltd., Nanjing, China) was cultured for 3–5 days in RPMI 1640 medium supplemented with 30% L929 cell supernatant to promote the growth of macrophages adherent to the culture surface. Mix fresh 1640 complete medium with CM of GPR91$^{-/-}$ or WT osteoblasts at a ratio of 1:1. Additionally, 20 ng/mL M-CSF (RP01216, AB clonal, China) and 50 ng/mL RANKL (RP00745, AB clonal, China) were added. They were then stained using a TRAP kit as instructed by the producer. The identification process involves counting the presence of three or more nuclei in a cell. Osteoclasts were counted as TRAP^{+} multinucleated osteoclast precursors, and images were recorded using an inverted microscope (Nikon, Japan).

Transwell migration assay

Transwell migration assay was done following the procedure described by Yang et al[50]. Osteoblasts from GPR91$^{-/-}$ or WT mice were separated in a serum-free medium, and cell numbers were adjusted to 2×10^5. The down chamber was occupied by 600 µl of complete medium containing 20% fetal calf serum. After a day of incubation at around 37 °C, nonmigrating cells were taken from the filter surface using cotton gauze. The drifted cells were fixed with 4% paraformaldehyde solution and then tarnished with 0.2% crystal violet solution (Service bio, G1014, China) for 10 min. The cells are then counted under the microscope.

Wound healing migration assay

4×10^6 Osteoblasts from GPR91$^{-/-}$or WT mice were plated into six-plates and cultured overnight. Linear scratches were prepared within the cell layer with the tip of a 200 µl pipetting tip when growth had reached 80% confluence; the cells were incubated with serum-free DMEM after being cleaned three times with PBS. The wound healing of cells in each group was photographed at 4× magnification after 0, 24, and 48 h of culture. Furthermore, the images were analyzed using Image J software, and the wound healing was compared at the exact location at different time points.

Western blot analysis

The western blot method described earlier was used[51]. Cell lysis was performed by applying ice-cold RIPA buffer (Beyotime Biotechnology, China). Following cell lysis, the protein amount was quantified by a nanodrop from Thermo Fisher Scientific, USA. Proteins splited by sodium dodecyl sulfate–polyacrylamide gel electrophoresis (SDS-PAGE) using the China Smart-Lifesciences system were drawn onto a polyvinylidene difluoride membrane from Millipore in the United States and then blocked with QuickBlock™ blocking buffer feeding through sealed China Beyotime Liquid. The membrane was blocked with 5% bovine albumin and then incubated with primary antibodies: OSX (1:1000; A18699, ABclonal, China), RUNX2 (1:1000; D1L7F, CST, Germany), OPN (1:1000; A21084, ABclonal, China), GPR91 (1:1000, orb157370, Biorbyt, China), RANKL (1:1000, 23408-1-AP, PTG, China), OPG (1:1000, DF6824, Affinity, China), TRAP (1:1000; A0962, ABclonal, China), MMP9 (1:1000; A11147, ABclonal, China), CCL2 (1:1000; A23288, ABclonal, China), P38 (1:1000; 8690, CST, Germany), p-P38 (1:1000; 4511, CST, Germany), JNK (1:1000; 9252, CST, Germany), p-JNK (1:1000; 4668, CST, Germany), p-P65 (1:1000, 93H1, CST, Germany), ERK (1:1000, GB11560, Servicebio, China), p-ERK (1:1000, AF1015, Affinity, China), β-actin (1:1000; 66009-l-lg, Proteintech, China). Followed by secondary antibodies (Thermo Fisher Scientific, USA). Protein bands were detected with ImageQuant LAS 4000.

Statistical analysis

The Shapiro–Wilk test was used to show the normality and the homogeneity of variants using the F test. Analysis of variance (ANOVA) and Dunnett's multiple comparisons for post hoc analysis analyzed experimental data. Two data sets were analyzed in different groups using a student's t-test, where a probability < 0.05 was considered significant. Results are expressed as mean ± SEM and analyzed using GraphPad Prism software (9.00).

Data availability

The datasets used and/or analyzed during the current study are available from the corresponding author upon reasonable request.

Received: 27 August 2024; Accepted: 5 November 2024
Published online: 11 November 2024

References

1. Bhuyan, R. et al. Periodontitis and its inflammatory changes linked to various systemic diseases: A review of its underlying mechanisms. *Biomedicines.* **10**(10), 2659 (2022).
2. Zhou, M. & Graves, D. T. Impact of the host response and osteoblast lineage cells on periodontal disease. *Front Immunol.* **13**, 998244 (2022).
3. Omi, M. & Mishina, Y. Roles of osteoclasts in alveolar bone remodeling. *Genesis.* **60**(8–9), e23490 (2022).
4. Hienz, S. A., Paliwal, S. & Ivanovski, S. Mechanisms of bone resorption in periodontitis. *J Immunol Res.* **2015**, 615486 (2015).
5. Zhang, J. R. et al. Different modulatory effects of IL-17, IL-22, and IL-23 on osteoblast differentiation. *Mediators Inflamm.* **2017**, 5950395 (2017).

6. Guo, C. et al. Lipopolysaccharide (LPS) induces the apoptosis and inhibits osteoblast differentiation through JNK pathway in MC3T3-E1 cells. *Inflammation.* **37**(2), 621–631 (2014).
7. Bostanci, N. & Belibasakis, G. N. Porphyromonas gingivalis: an invasive and evasive opportunistic oral pathogen. *FEMS Microbiol Lett.* **333**(1), 1–9 (2012).
8. Lunar Silva, I. & Cascales, E. Molecular Strategies Underlying Porphyromonas gingivalis Virulence. *J Mol Biol.* **433**(7), 166836 (2021).
9. Chen, H. et al. Highly multiplexed bioactivity screening reveals human and microbiota metabolome-GPCRome interactions. *Cell* **186**, 3095-3110.e19 (2023).
10. Murakami, N. et al. Butyric acid modulates periodontal nociception in Porphyromonas gingivalis-induced periodontitis. *J Oral Sci* **64**, 91–94 (2022).
11. Zhang, D., Li, S., Hu, L., Sheng, L. & Chen, L. Modulation of protease-activated receptor expression by Porphyromonas gingivalis in human gingival epithelial cells. *BMC Oral Health* **15**, 128 (2015).
12. Wettschureck, N. & Offermanns, S. Mammalian G proteins and their cell type specific functions. *Physiol Rev.* **85**(4), 1159–1204 (2005).
13. Rubić-Schneider, T. et al. GPR91 deficiency exacerbates allergic contact dermatitis while reducing arthritic disease in mice. *Allergy.* **72**(3), 444–452 (2017).
14. Guo, Y. et al. Succinate and its G-protein-coupled receptor stimulates osteoclastogenesis. *Nat Commun.* **8**, 15621 (2017).
15. Guo, Y. et al. Targeting the succinate receptor effectively inhibits periodontitis. *Cell Rep.* **40**(12), 111389 (2022).
16. Thiel, A. et al. Osteoblast migration in vertebrate bone. *Biol Rev Camb Philos Soc.* **93**(1), 350–363 (2018).
17. Krzak, G., Willis, C. M., Smith, J. A., Pluchino, S. & Peruzzotti-Jametti, L. Succinate receptor 1: An emerging regulator of myeloid cell function in inflammation. *Trends Immunol.* **42**(1), 45–58 (2021).
18. Byrne, S. J. et al. Progression of chronic periodontitis can be predicted by the levels of Porphyromonas gingivalis and Treponema denticola in subgingival plaque. *Oral Microbiol Immunol.* **24**(6), 469–477 (2009).
19. Loomer, P. M., Sigusch, B., Sukhu, B., Ellen, R. P. & Tenenbaum, H. C. Direct effects of metabolic products and sonicated extracts of Porphyromonas gingivalis 2561 on osteogenesis in vitro. *Infect Immun.* **62**(4), 1289–1297 (1994).
20. Kim, C. S. et al. The effect of recombinant human bone morphogenetic protein-4 on the osteoblastic differentiation of mouse calvarial cells affected by Porphyromonas gingivalis. *J Periodontol.* **73**(10), 1126–1132 (2002).
21. Azuma, H., Kido, J., Ikedo, D., Kataoka, M. & Nagata, T. Substance P enhances the inhibition of osteoblastic cell differentiation induced by lipopolysaccharide from Porphyromonas gingivalis. *J Periodontol.* **75**(7), 974–981 (2004).
22. Kato, T. et al. Porphyromonas gingivalis gingipains cause G(1) arrest in osteoblastic/stromal cells. *Oral Microbiol Immunol.* **23**(2), 158–164 (2008).
23. Kang, M. S., Moon, J. H., Park, S. C., Jang, Y. P. & Choung, S. Y. Spirulina maxima reduces inflammation and alveolar bone loss in Porphyromonas gingivalis-induced periodontitis. *Phytomedicine.* **81**, 153420 (2021).
24. Zhang, W., Ju, J., Rigney, T. & Tribble, G. Porphyromonas gingivalis infection increases osteoclastic bone resorption and osteoblastic bone formation in a periodontitis mouse model. *BMC Oral Health.* **14**, 89 (2014).
25. Shiau, H. J., Aichelmann-Reidy, M. E. & Reynolds, M. A. Influence of sex steroids on inflammation and bone metabolism. *Periodontol 2000* **64**(1), 81–94 (2014).
26. Shiau, H. J. & Reynolds, M. A. Sex differences in destructive periodontal disease: A systematic review. *J Periodontol.* **81**(10), 1379–1389 (2010).
27. Rubic, T. et al. Triggering the succinate receptor GPR91 on dendritic cells enhances immunity. *Nat Immunol.* **9**(11), 1261–1269 (2008).
28. Peruzzi, B. et al. c-Src and IL-6 inhibit osteoblast differentiation and integrate IGFBP5 signalling. *Nat Commun.* **3**, 630 (2012).
29. Komori, T. Regulation of bone development and extracellular matrix protein genes by RUNX2. *Cell Tissue Res.* **339**(1), 189–195 (2010).
30. Lee, M., Arikawa, K. & Nagahama, F. Micromolar levels of sodium fluoride promote osteoblast differentiation through Runx2 signaling. *Biol Trace Elem Res.* **178**(2), 283–291 (2017).
31. Kusuyama, J. et al. JNK inactivation suppresses osteogenic differentiation, but robustly induces osteopontin expression in osteoblasts through the induction of inhibitor of DNA binding 4 (Id4). *FASEB J.* **33**(6), 7331–7347 (2019).
32. Fakhry, M., Hamade, E., Badran, B., Buchet, R. & Magne, D. Molecular mechanisms of mesenchymal stem cell differentiation towards osteoblasts. *World J Stem Cells.* **5**(4), 136–148 (2013).
33. AlQranei, M. S., Senbanjo, L. T., Aljohani, H., Hamza, T. & Chellaiah, M. A. Lipopolysaccharide- TLR-4 Axis regulates Osteoclastogenesis independent of RANKL/RANK signaling. *BMC Immunol.* **22**(1), 23 (2021).
34. Okahashi, N. et al. Porphyromonas gingivalis induces receptor activator of NF-kappaB ligand expression in osteoblasts through the activator protein 1 pathway. *Infect Immun.* **72**(3), 1706–1714 (2004).
35. Kong, Y. Y. et al. OPGL is a key regulator of osteoclastogenesis, lymphocyte development and lymph-node organogenesis. *Nature.* **397**(6717), 315–323 (1999).
36. Hayman, A. R. Tartrate-resistant acid phosphatase (TRAP) and the osteoclast/immune cell dichotomy. *Autoimmunity* **41**, 218–223 (2008).
37. Yun, H. M., Kim, B., Park, J. E. & Park, K. R. Trifloroside induces bioactive effects on differentiation, adhesion, migration, and mineralization in pre-osteoblast MC3T3E-1 cells. *Cells.* **11**(23), 3887 (2022).
38. Mao, H., Yang, A., Zhao, Y., Lei, L. & Li, H. Succinate supplement elicited "pseudohypoxia" condition to promote proliferation, migration, and osteogenesis of periodontal ligament cells. *Stem Cells Int.* **2020**, 2016809 (2020).
39. Bartlett, J. D. & Smith, C. E. Modulation of cell-cell junctional complexes by matrix metalloproteinases. *J Dent Res.* **92**(1), 10–17 (2013).
40. Duncan, H. F. et al. The histone-deacetylase-inhibitor suberoylanilide hydroxamic acid promotes dental pulp repair mechanisms through modulation of matrix metalloproteinase-13 activity. *J Cell Physiol.* **231**(4), 798–816 (2016).
41. Deng, G. et al. Inhibition of cancer cell migration with CuS@ mSiO(2)-PEG nanoparticles by repressing MMP-2/MMP-9 expression. *Int J Nanomedicine.* **13**, 103–116 (2018).
42. Ko, S. H. et al. Succinate promotes stem cell migration through the GPR91-dependent regulation of DRP1-mediated mitochondrial fission. *Sci Rep.* **7**(1), 12582 (2017).
43. Liu, L., Tang, W., Wu, S., Ma, J. & Wei, K. Pulmonary succinate receptor 1 elevation in high-fat diet mice exacerbates lipopolysaccharides-induced acute lung injury via sensing succinate. *Biochim Biophys Acta Mol Basis Dis* **1870**, 167119 (2024).
44. Hah, Y. S. et al. JNK signaling plays an important role in the effects of TNF-α and IL-1β on in vitro osteoblastic differentiation of cultured human periosteal-derived cells. *Mol Biol Rep.* **40**(8), 4869–4881 (2013).
45. Rodríguez-Carballo, E., Gámez, B. & Ventura, F. p38 MAPK signaling in osteoblast differentiation. *Front Cell Dev Biol.* **4**, 40 (2016).
46. Kim, J. M. et al. The ERK MAPK pathway is essential for skeletal development and homeostasis. *Int J Mol Sci.* **20**(8), 1803 (2019).
47. Greenblatt, M. B., Shim, J. H. & Glimcher, L. H. Mitogen-activated protein kinase pathways in osteoblasts. *Annu Rev Cell Dev Biol.* **29**, 63–79 (2013).
48. Atallah R, Olschewski A, Heinemann A. Succinate at the crossroad of metabolism and angiogenesis: Roles of SDH, HIF1α and SUCNR1. *Biomedicines.* 2022. 10(12).

49. Yu, Y., Jiang, L., Li, J., Lei, L. & Li, H. Hexokinase 2-mediated glycolysis promotes receptor activator of NF-κB ligand expression in Porphyromonas gingivalis lipopolysaccharide-treated osteoblasts. *J Periodontol.* **93**(7), 1036–1047 (2022).
50. Yang, Y. et al. Compressive force regulates cementoblast migration via downregulation of autophagy. *J Periodontol.* **92**(11), 128–138 (2021).
51. Su, W. et al. Porphyromonas gingivalis triggers inflammatory responses in periodontal ligament cells by succinate-succinate dehydrogenase-HIF-1α axis. *Biochem Biophys Res Commun.* **522**(1), 184–190 (2020).

Acknowledgements
This research was partly supported by the National Natural Science Foundation of China (No. 82371007) and the Postgraduate Research & Practice Innovation Program of Jiangsu Province (KYCX23_0196).

Author contributions
Wenqi Su: Methodology; data curation; formal analysis; investigation; writing – original draft. Dandan Zhang: Methodology; validation. Yujia Wang: Methodology; software. Lang Lei: Writing – review and editing; supervision. Houxuan Li: Conceptualization; writing – review and editing; funding acquisition; methodology; supervision.

Declarations

Competing interests
The authors declare no competing interests.

Ethical approval
Each author has read and passed the final version and reached an agreement to ensure all features of the work are accurate.

Additional information
Supplementary Information The online version contains supplementary material available at https://doi.org/10.1038/s41598-024-78944-9.

Correspondence and requests for materials should be addressed to H.L.

Reprints and permissions information is available at www.nature.com/reprints.

Publisher's note Springer Nature remains neutral with regard to jurisdictional claims in published maps and institutional affiliations.